A multiscale modeling approach to fatigue damage in discontinuous fiber polymer composites[1]

Ba Nghiep Nguyen*, Brian J. Tucker, Mohammad A. Khaleel

Pacific Northwest National Laboratory, PO Box 999, Richland, WA 99352, USA

Abstract

The damage process in composite materials occurs at different length scales, ranging from the scale of the constituents and defects (*microscale*) to that of a composite structure (*macroscale*). This paper develops a multi-scale mechanistic approach to fatigue damage in discontinuous-fiber polymer composites. The approach accounts for the damage mechanisms in addition to the constituents' properties and characteristics. It links these micro-features to the behavior of the composite structure through a series of scale transitions using computational techniques that are based on micromechanical modeling, a thermodynamics-based formulation and finite element analysis.

Keywords: Multiscale modeling; Fatigue; Damage; Discontinuous fiber composites; Matrix cracking; Fiber/matrix debonding

1. Introduction

In order to use discontinuous fiber polymer composites for structural or semi-structural automotive applications, it is essential to understand and predict their fatigue behavior under cyclic loading conditions. This paper addresses fatigue damage in these materials by means of a multiscale mechanistic approach. At the *microscale*, the progressive damage mechanisms such as *matrix microcracking* and *fiber/matrix debonding* responsible for the reduction of the composite stiffness and strength are analyzed, and the associated damage variables are then defined. Next, the modified Mori–Tanaka model [1] and the average orientation distribution of fibers and microcracks are used to determine the stiffness of the composite (*mesoscale*) affected by these damage mechanisms [2]. After that, the constitutive relations and the damage evolution law are determined using a thermodynamics-based formulation, which extends the Thionnet–Renard fatigue model [3] for continuous fiber composites to random discontinuous fiber composites. Static damage depends only on the loading level, material properties, and characteristics, whereas fatigue damage is not only dependent on these factors, but is also a function of the number of cycles, frequency, the maximum and minimum values of the applied stress, etc. Therefore, it is necessary to account for these additional parameters to determine how damage can be accumulated under cyclic loading. Finally, the implementation of the fatigue damage model into the ABAQUS finite element code provides an effective and practical tool for the analysis and design of discontinuous fiber composite structures (*macroscale*) in terms of fatigue lifetime. The model has been validated using the experimental data found in [4].

2. Stiffness reduction law

Since the damage mechanisms that occur in a discontinuous fiber polymer composite subjected to quasi-static loads are the same as those for cyclic loads, the stiffness reduction law for the composite is the same for both loading conditions. This section summarizes our previous work to establish the stiffness reduction law for these materials [2]. The damage process has two stages. The first stage involves mainly matrix cracking coupled with fiber/matrix debonding, while the second stage corresponds to failure of the composite characterized by excessive matrix cracking and fiber/matrix debonding that lead to fiber pull-out and rupture.

In [2], Nguyen et al. consider a *reference composite* which contains unidirectional fiber tows (or fibers) and

* Corresponding author. Tel.: +1 (509) 375 3634; Fax: +1 (509) 375 6736; E-mail: ba.nguyen@pnl.gov

Computational Fluid and Solid Mechanics 2005
K.J. Bathe (Editor)

fiber-shape matrix microcracks in addition to imperfectly bonded fiber/matrix interfaces. Matrix microcracks were modeled as the second inclusion phase of zero stiffness. Consequently, the limit of the modified Mori–Tanaka solution proposed by Qu [1] for the microcrack stiffness tending towards zero value allowed the stiffness of the reference composite to be determined [2]:

$$\begin{aligned} \boldsymbol{C} = \lim(& f_m \boldsymbol{C}_m + f_1 \boldsymbol{C}_1 : \boldsymbol{A}_1 + f_2 \boldsymbol{C}_2 : \boldsymbol{A}_2) : \\ & (f_m \boldsymbol{I} + f_1 \boldsymbol{A}_1 + f_2 \boldsymbol{A}_2 + f_1 \boldsymbol{H}_1 : \boldsymbol{C}_1 : \boldsymbol{A}_1 + f_2 \boldsymbol{H}_2 : \boldsymbol{C}_2 : \boldsymbol{A}_2) \\ & \boldsymbol{C}_2 \to 0 \end{aligned} \tag{1}$$

where $\boldsymbol{C}_m$ and $\boldsymbol{C}_i$ $(i = 1, 2)$ are the stiffness tensors of the matrix and inclusions, respectively. A_i denote the inclusion concentration matrices which are expressed in terms of the modified Eshelby tensor defined by [1]. This tensor accounts for the imperfectly bonded fiber/matrix interfaces through a related-compliance tensor of the interfaces.

The matrix microcrack volume fraction f_2 is used as the damage variable describing matrix cracking, and it is renamed as 'α', while a second damage variable governing the compliance of the fiber/matrix interfaces is defined as:

$$\beta = \beta(r, E_m, \beta^*) = \frac{r\beta^*}{E_m} \tag{2}$$

where r is the fiber radius, and E_m is the matrix elastic modulus. β^* is linked to the participation rate of fiber/matrix debonding in the damage process and is the damage variable associated with this mechanism. β^* varies from 0 to β^*_L. The 0 value represents a perfectly bonded interface while advanced stages of degradation approaching complete debonding is characterized by $\beta^* = \beta^*_L$. Since matrix cracking is coupled with interfacial debonding, the relation: $\beta^* = \beta^*(\alpha)$ needs to be established experimentally. A procedure using acoustic emission techniques is given in [2].

The stiffness of the random fiber composite containing random matrix microcracks and imperfect fiber/matrix interfaces is computed from the stiffness of the reference composite given by Eq. (1), which is averaged over all possible orientations and weighted by Karcir et al.'s [5] orientation distribution function [2,6]:

$$\bar{\boldsymbol{C}}[\alpha, \beta^*(\alpha)] = \bar{\boldsymbol{C}}(\alpha) = \frac{\int_{-\pi/2}^{0} \boldsymbol{R}(\alpha,\theta)\lambda e^{-\lambda(-\theta)} d\theta + \int_{0}^{\pi/2} \boldsymbol{R}(\alpha,\theta)\lambda e^{-\lambda\theta} d\theta}{2\int_{0}^{\pi/2} \lambda e^{-\lambda\theta} d\theta} \tag{3}$$

$\boldsymbol{R}(\alpha, \theta)$ is the global stiffness matrix of the reference composite, which is obtained by transforming $\boldsymbol{C}(\alpha)$ into the global coordinate system. Considering planar orientations, the global coordinate system is defined such that the fibers and microcracks are in the 1–2 plane with the orientation angle θ measured from the 1-axis.

3. Constitutive and damage evolution relations

Damage due to cyclic loads results from *static damage* plus the accumulated *fatigue damage*. This section extends the thermodynamics-based formulation used in [3] for laminated continuous fiber composites to discontinuous fiber composites containing distributions of microcracks and subjected to cyclic loading. This formulation uses a thermodynamic potential (which is the elastic deformation energy), Clausius–Duhem's inequality (dissipation criterion), and a damage criterion. The thermodynamic potential is expressed in terms of independent state variables. The constitutive relations are obtained by deriving the thermodynamic potential with respect to the strains:

$$\sigma_i = \frac{\partial \phi(\varepsilon_i, \alpha)}{\partial \varepsilon_i} = \bar{C}_{ij}(\alpha)\varepsilon_j \tag{4}$$

where $\bar{C}_{ij}(\alpha)$ is given by Eq. (3).

Under cyclic loading conditions, the damage criterion (Eq. (5)) depends on a damage threshold F_c which is a function of the *key loading parameters* such as the *number of cycles N*, the *maximum stress* σ_{max} within a cycle, the *ratio of the minimum-to-maximum stresses R*, and the *frequency* ω:

$$f(F, \alpha) = F_c(\alpha, N, \sigma_{max}, R, \omega) - F(\varepsilon_{ij}, \alpha) \le 0 \tag{5}$$

Among these parameters, the number of cycles is used as a variable in addition to the independent damage variable α to describe the damage evolution. The other parameters are treated as constants during the prescribed cyclic loads. In (5), the thermodynamic force F associated with α is obtained by deriving the thermodynamic potential with respect to this damage variable. The damage threshold function can be determined by using the experimental crack density data as a function of the number of cycles for the prescribed, σ_{max}, R and ω. Finally, the damage evolution law is obtained using criterion (5) and the consistency conditions ($f = 0$ and $df = 0$):

$$d\alpha = -\frac{\frac{d\bar{C}_{ij}}{d\alpha}\varepsilon_i d\varepsilon_j}{\frac{1}{2}\frac{d^2\bar{C}_{ij}}{d\alpha^2}\varepsilon_i\varepsilon_j - \frac{\partial F_c}{\partial\alpha}} + \frac{\frac{\partial F_c}{\partial N} dN}{\frac{1}{2}\frac{d^2\bar{C}_{ij}}{d\alpha^2}\varepsilon_i\varepsilon_j - \frac{\partial F_c}{\partial\alpha}} \tag{6}$$

The first term of the right-hand side of (6) represents the contribution of quasi-static damage while the second term accounts for fatigue damage due to the increase in the number of cycles.

4. Applications

The computational procedure has two parts. The first part determines the initial elastic properties, the stiffness reduction parameters and the parameters of the damage threshold function. The second part is related to the finite element analysis using ABAQUS. The user subroutine UMAT of this code was employed to implement the constitutive relations and damage evolution law. In a quasi-static damage analysis, the loads are incrementally applied whereas in a fatigue damage problem, the number of cycles is incremented. The other loading parameters ($\sigma_{\max}$, R and ω) are kept constant and constitute the loading characteristics.

The random glass/polyester composite studied in [4] is used in this paper for the model validation. The number of acoustic emission (AE) events versus AE signal amplitudes in [4] for this material was used and converted into the crack density data needed to compute the damage threshold function under the loading conditions characterized by: $R = 0.2$, $\sigma_{\max} = 0.31\sigma_{\text{fail}} = 45$ MPa, and $\omega = 5$ Hz. Figure 1 relates the experimental and predicted crack density evolutions to the number of cycles. Very good agreement of results has been found. Figure 1 shows three phases of the crack density evolution. The first phase for $N = 0$ is purely due to the quasi-static damage contribution caused by loading the composite to $\sigma_{\max}$. The second phase is characterized by a smooth and slow evolution of the crack density with the number of cycles. This phase should be rendered as long as possible to maximize the lifetime of the composite. The third and final phase corresponds to a dramatic increase in crack density with a small increase in the number of cycles resulting in catastrophic failure.

Finally, the model was used to determine damage accumulations in a random glass/polyester plate containing a central hole and under cyclic loading with $\omega = 5$ Hz, $R = 0.2$, and $\sigma_{\max} = 10$ MPa applied at one plate end. The same material was considered as before. The remote applied stress has produced a maximum longitudinal stress of 45MPa around the circular edges of the hole (Fig. 2), and consequently, quasi-static damage and fatigue damage are much greater in those areas than in other regions. Figure 3(a) and (b) show the damage distributions in the plate after 40 000 and 115 000 cycles, respectively. Macroscopic cracks are predicted to initiate from the hole when the microcrack density has attained the saturation value.

5. Conclusion

This paper has described a multiscale modeling approach for predicting fatigue damage in discontinuous

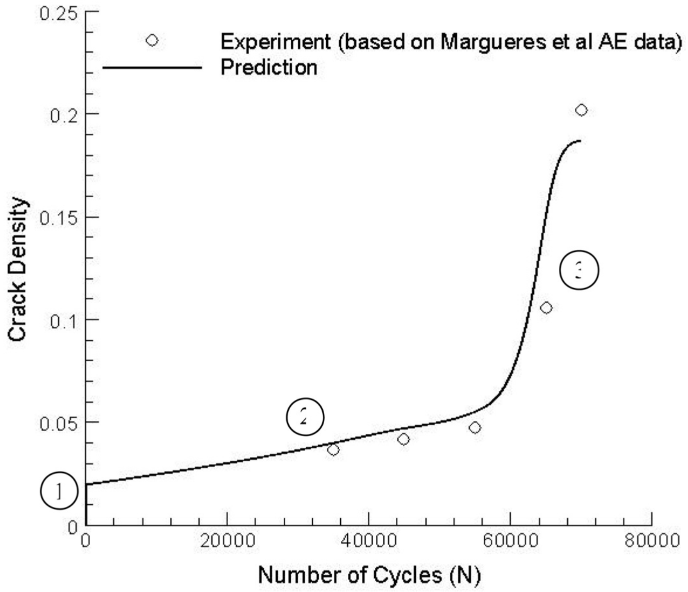

Fig. 1. Measured and predicted crack density versus number of cycles for a random discontinuous glass/polyester composite. The experimental values were determined from the AE data from [4]. 1, 2 and 3 denote three phases of the damage development.

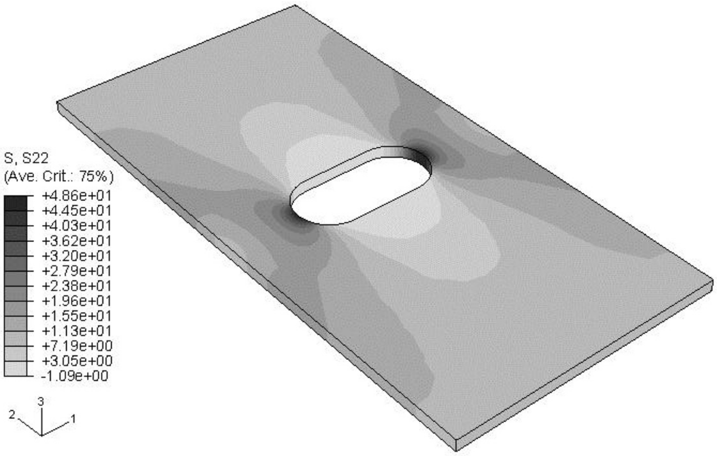

Fig. 2. Contour of the longitudinal stresses resulting from the maximum remote applied stress of $\sigma_{\max} = 10$ MPa.

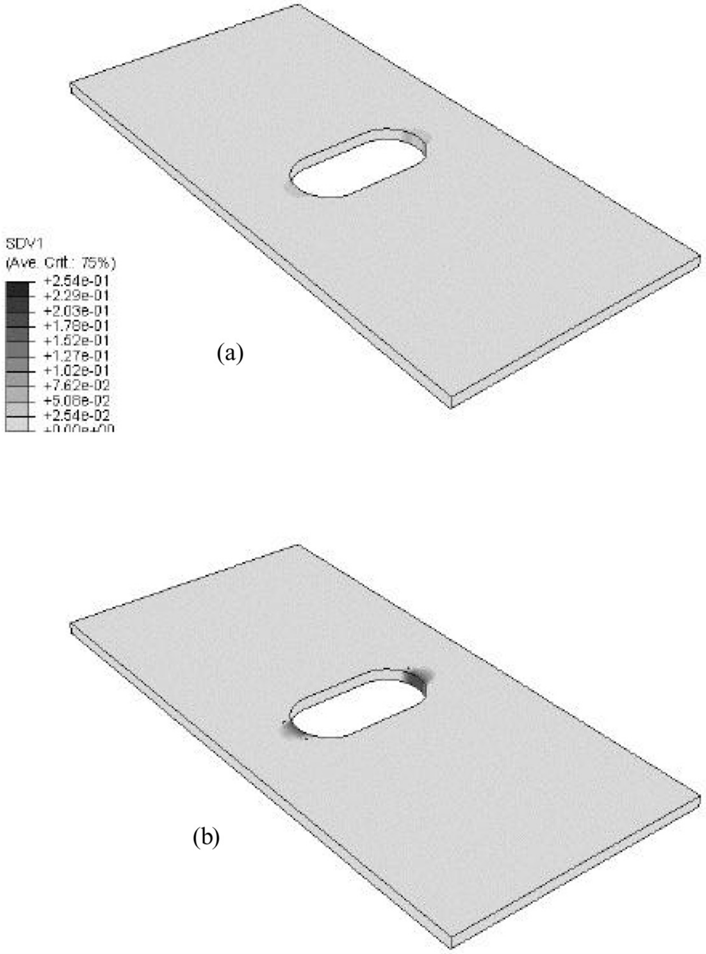

Fig. 3. Predicted fatigue damage progression for a random glass/polyester plate containing a central hole after 4×10^4 (a) and 1.15×10^5 (b) cycles under $\sigma_{\text{applied}}^{\max} = 10$ MPa, *Frequency* = *5* Hz.

fiber polymer composites ranging from the scale of the constituents and micro-defects to the scale of a composite structure. The scale transitions were carried out using micromechanics, continuum damage mechanics and thermodynamics of continuous media. The model implementation into ABAQUS has enabled a fatigue damage analysis for a random glass/polyester plate containing a central hole and subjected to cyclic loading. It is noted that the model can be extended to multi-level fatigue stresses, and this offers the potential to apply the model in other practical engineering applications.

Notes

[1] This manuscript has been authored by Battelle Memorial Institute, Pacific Northwest Division, under Contract No. DE-AC06-76RL0 1830 with the US Department of Energy. The United States Government retains and the publisher, by accepting the article for publication, acknowledges that the United States Government retains a non-exclusive, paid-up, irrevocable, world-wide license to publish or reproduce the published form of this manuscript, or allow others to do so, for United States Government purposes.

References

[1] Qu J. The effect of slightly weakened interfaces on the overall elastic properties of composite materials. Mech of Mat 1993;14:269–281.

[2] Nguyen BN, Tucker BJ, Khaleel MA. Damage in short-fiber composites: from the microscale to the continuum solid. In: Proceedings of the 2004 ASME International Mechanical Engineering Congress (IMECE 2004), Paper No. IMECE2004-59129, 13–19 November, 2004, Anaheim, CA.

[3] Thionnet A, Renard J. Laminated composites under fatigue loading: a damage development law for transverse cracking. Comp Sci and Tech 1994;52:173–181.

[4] Margueres P, Meraghni F, Benzeggagh ML. Comparison of stiffness measurements and damage investigation techniques for a fatigued and post-impact fatigued GFRP composite obtained by RTM process. Composites – Part A: Applied Science and Manufacturing 2000;31:151–163.

[5] Karcir L, Narkis M, Ishai O. Oriented short glass-fiber composites: I preparation and statistical analysis of aligned fiber materials. Polymer Eng Sci 1975;15:525–531.

[6] Nguyen BN, Khaleel MA. A mechanistic approach to damage in short-fiber composites based on micromechanical and continuum damage mechanics descriptions. Comp Sci and Tech 2004;64:607–617.